

Estimation of evapotranspiration in northeastern Mongolia combining satellite data and ground data

MATSUURA Yosuke¹, and MATSUSHIMA Dai¹

¹ Department of Geophysics, Graduate School of Science, Tohoku University, Sendai, Japan

Key words: evapotranspiration, land coverage, pattern decomposition method

I Introduction

The climate of Mongolia is characterized by a dry-cold term and a wet-hot term. In such condition the activity of vegetation changes dramatically through a year. Evapotranspiration is one of the most important elements in water cycle, especially in arid area. In order to research the water cycle, it is important to quantify the amount of evapotranspiration. In this study, by using MODIS data and 4 automatic weather station (AWS) data, seasonal change of evapotranspiration in year 2003 is investigated.

II Methods

1. Study area

The subject area of this study is a transition area of Kherlen River basin in northeastern Mongolia, where the vegetation changes from northern forest region to southern arid region. The segment for present analysis is divided between latitudes 46° N and 48° N and longitudes 108° E and 111° E. Annual mean temperature is about -2 °C, and the range of temperature change is as large as 50 °C in a year. Annual precipitation is about 200 mm, and most of which fall during summer.

2. Satellite data

We use the Moderate-Resolution Imaging Spectroradiometer (MODIS) sensor in the “Terra” satellite which was launched by NASA in December 1999. The MODIS sensor has 36 bands from visible to thermal infrared parts of the electromagnetic spectrum. And it provides global observation data every day from a mean altitude of 705 km. It passes and scans over Mongolia at about 11:30 a.m. (±1 hour) LST.

3. Pattern decomposition method

We use 6 bands of visible and near-infrared parts (Table 1) whose highest spatial resolution is 500 m. One pixel can include many types of land cover, which is called “mixed pixels”, and a spectrum of a “mixed pixels” is considered as a superposition of basic spectrum patterns, which corresponds to land cover elements. Using pattern decomposition method, the mixed spectrum can be decomposed into basic spectrum patterns (Muramatsu *et al.*, 2000). In this study three land covers, “water”, “vegetation”, and “soil” are adopted as basic land covers as follows:

$$A_i = c_w P_{iw} + c_v P_{iv} + c_s P_{is} \quad (1)$$

where A_i is a spectrum pattern in the reference pixel. c_w , c_v and c_s are the ratio of each land area in the reference pixel. P_w , P_v and P_s are water, vegetation and soil spectrum pattern, respectively (Fig. 1). The ratios are calculated using the least-squares method as

$$\kappa^2 = \sum_{i=1}^6 [A_i - (c_w P_{iw} + c_v P_{iv} + c_s P_{is})]^2 \quad (2)$$

A combination of the land area ratios is determined when κ^2 is minimum with the conditions $c_w \geq 0$, $c_v \geq 0$ and $c_s \geq 0$. To estimate the accuracy, the relative error (ΔA) is defined as

$$\Delta A = \sqrt{\kappa^2} / \sum_{i=1}^6 A_i \quad (3)$$

In order to make the sum of the three fractions unity, three land area ratios are normalized as follows:

$$c_k \approx c_k / (c_w + c_v + c_s) \quad k = w, v, s \quad (4)$$

When the pattern decomposition method is applied to the subject area the ratio of water area c_w tends to be overestimated. This is caused by the noise such as shade, which mainly appears in c_w because water spectrum pattern P_w is comparatively small. To avoid the difficulty, we make a database of places where there is a possibility of water surface by extracting pixels whose reflectance is very small. In such places we apply “three land coverage” pattern decomposition method. The other places are applied “two land coverage” pattern decomposition method with $c_w = 0$.

4. Observing data

Meteorological data have been observed in 4 AWS since March 25th, 2003. They are available for bulk formulae. Whereas during intensive observing period (IOP, one day per one month for each AWS), some meteorological data, wind speed and air temperature for example, are observed with a high frequency (10 Hz), which are available for eddy-correlation method. Some parameters in bulk formulae are unknown. So, they need to be quantified through equating estimations of those two ways. The detail is as follows.

5. Parameterization of evapotranspiration

Table 1 Spectrum bands used in this study.

| Band | Wavelength range |
|------|------------------|
| 1 | 620 ~ 670 nm |
| 2 | 841 ~ 876 nm |
| 3 | 459 ~ 479 nm |
| 4 | 545 ~ 565 nm |
| 5 | 1628 ~ 1652 nm |
| 6 | 2105 ~ 2155 nm |

Table 2 List of the AWS site and precipitation there in July and October.

| Band | Wavelength range |
|------|------------------|
| 1 | 620 ~ 670 nm |
| 2 | 841 ~ 876 nm |
| 3 | 459 ~ 479 nm |
| 4 | 545 ~ 565 nm |
| 5 | 1628 ~ 1652 nm |
| 6 | 2105 ~ 2155 nm |

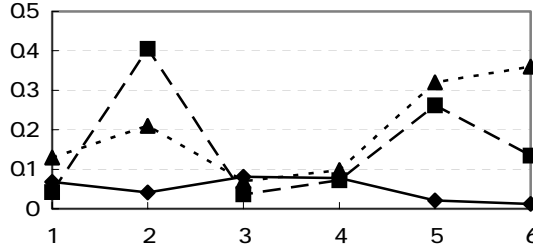


Fig. 1 Basic spectrum patterns for each land cover.

— water - - vegetation soil

The bulk formula for estimating water vapor flux (E) is given as

$$E = \rho\beta C_H U (q_{sat} - q) \quad (5)$$

where ρ is air density, β evaporation efficiency, C_H bulk transfer coefficient, U wind speed, q_{sat} specific humidity at saturation, which depends on surface temperature (T_s) and is q specific humidity.

5.1 Bulk transfer coefficient

Sensible heat flux (H) can be formulated in two ways. One of which is eddy-correlation method

$$H = \rho c_p \overline{w' T_a'} \quad (6)$$

and the other is the bulk formula

$$H = \rho c_p C_H (T_s - T_a) \quad (7)$$

where c_p is isobaric specific heat of the atmosphere, w' is the perturbation of vertical wind speed, T_a and T_a' are air temperature and its perturbation, respectively. We compared the estimations of sensible heat flux between eqs. (6) and (7), and learned that we could consider it as constant value through a month, 0.0017 and 0.0013 in July and October, respectively.

5.2 Evaporation efficiency

Water vapor flux is estimated by using eddy- correlation

method as follows:

$$E = \overline{\rho w' q'} \quad (8)$$

where q' is the perturbation of specific humidity. The energy balance equation is as follows:

$$S^\downarrow (1 - a) + L^\downarrow - \sigma T_s^4 - G = H + tE \quad (9)$$

where $S^\downarrow, L^\downarrow, G$ are downward short-wave radiation, downward long-wave radiation, and soil heat flux, respectively. a is surface albedo, σ the Stefan-Boltzman constant, and t the latent heat of evaporation. Substituting eqs. (6) and (8) into eq. (9), eq. (9) can be solved by T_s . Evaporation efficiency is determined, minimizing difference between the estimation of eq. (5) and eq. (8). Estimation by the eddy-correlation method during IOP is given by Kojima (2004). With them we find out what β depends on.

5.3 Surface temperature

After quantifying β by using eddy-correlation method, we can estimate T_s through bulk formulae instead of eddy-correlation method. Substituting eqs. (5) and (7), eq. (9) is written as:

$$\begin{aligned} S^\downarrow (1 - a) + L^\downarrow - \sigma T_s^4 - G \\ = \rho c_p C_H U (T_s - T_a) + t \rho \beta C_H U (q_{sat} - q) \end{aligned} \quad (10)$$

When we apply eq. (10) to places other than the AWS, meteorological data are interpolated which are weighed with the distances from the AWS. Indeed, this approach is inappropriate to evaluate the amount of an instantaneous evapotranspiration. However, it is appropriate if we evaluate that of a monthly evapotranspiration because the locality weakens.

Finally, the amount of evapotranspiration is estimated as follows:

$$E = c_w E_w + (c_v + c_s) E_g \quad (11)$$

where E_w , E_g are evapotranspiration from water surface and grassland estimated by eq. (5) with appropriate parameters, respectively.

III Results and discussion

1. Pattern decomposition method to MODIS data

Fig. 2 shows the output of the pattern decomposition method applied to data on July 28th. The transition of vegetation from north to south and some springs around Kherlen River are found.

The average relative error for all samples is 20%. Most of the large relative error appear in low-reflectance area such as forest and places near clouds, where noise become relatively large because of their shade. The other places are thought to be well decomposed, with the correlation between c_v and NDVI larger than 0.9.

2. Relation between evaporation efficiency and the amount of vegetation

Evaporation efficiency is divided into two terms as follows:

$$\beta = \frac{1}{1 + C_H UF(\theta) / D_{atm}} + \frac{1}{C_H U r_v} \quad (12)$$

where D_{atm} is the molecular diffusion coefficient of water vapor, F a empirical function which depends on volumetric water content (θ) and soil property, and an resistance of water flow inside plants. The first term of right-side stands for the evaporation from soil (Kondo *et al.*, 1990), and the second term stands for the transpiration from vegetation. We examined the relation between r_v and c_v through comparing the estimations of water vapor flux between eqs. (5) and (8), and obtained the inversely proportional relation (Fig. 3) as follows:

$$r_v = 146 / c_v \quad (13)$$

For example, the first term of right-side is about 0.02 with the condition $\theta = 0.04$ and the second term is about 0.15 over grassland in summer. Whereas the second term over bare soil is 0, of course.

3. Estimation of a monthly evapotranspiration

We suppose that each land cover ratio keeps constant through a month. eq. (11) was applied to the data on July 28th, substituting daily average meteorological data for eq. (5). Fig. 4a shows the amount of a monthly evapotranspiration in July. Generally speaking, about 100 mm of water evaporates over water surface, while 50 mm evaporates from grassland, which are larger than 90% of precipitation (see Table 2).

We applied the same process to the data in October. To estimate the ratio of land area we used MODIS data on October 17th. Fig. 4b shows the amount of a monthly evapotranspiration in October. There is very little vegetation and much less precipitation. Hence, the amount of a monthly evapotranspiration in October is

much smaller than that in July. However, it can also be said that most of precipitation evaporates back to the atmosphere.

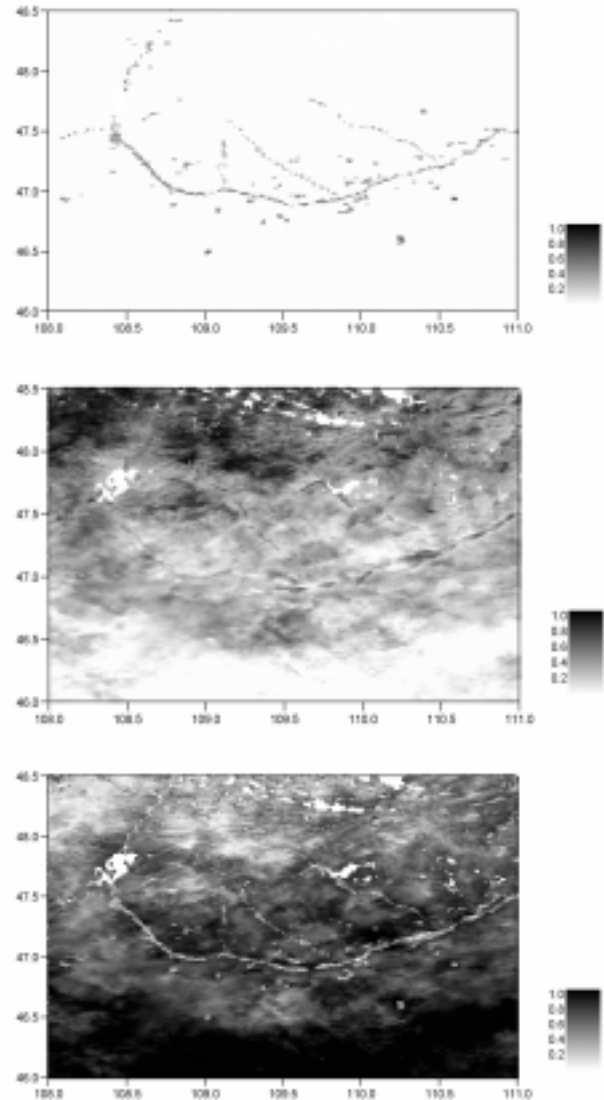


Fig. 2 Pattern decomposition method for MODIS data on July 28th.
Top...water middle...vegetation bottom...soil

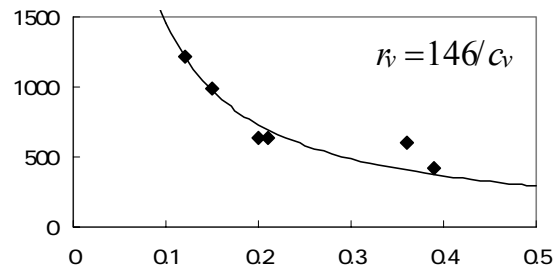


Fig. 3 Relation between c_v and r_v .

IV Conclusions

Pattern decomposition method was applied with MODIS data in northeastern Mongolia on July 28th and October 17th, 2003. And we succeeded in detecting the surface conditions.

We parameterized water vapor flux over grassland and found that transpiration was more dominant than evaporation in amount while vegetation was active.

We estimated the distribution of the amount of a monthly evapotranspiration in July and October. These two months are quite different in amount because of the difference of a vegetation ratio as well as that of a soil moisture. A seasonal change mainly depends on these two elements. In any case, more than 90% of precipitation evaporates back to the atmosphere.

References

- Kojima, T. (2004): An analysis what causes are dominant on evapotranspiration in Kherlen River basin, Mongolia. *M. S. Thesis, University of Tsukuba.*
- Kondo, J., Saigusa, N. and Sato, T. (1990): A Parameterization of Evaporation from Bare Soil Surfaces. *Reprinted from JOURNAL OF APPLIED METEOROLOGY*, **29**, 385-389.
- Muramatsu, K., Furumi, S., Fujiwara, N., Hayashi, A., Daigo, M. and Ochiai, F. (2000): Patterndecomposition method in the albedo space for Landsat TM and MSS data analysis. *International Journal of Remote Sensing*, **21**, 99-119.

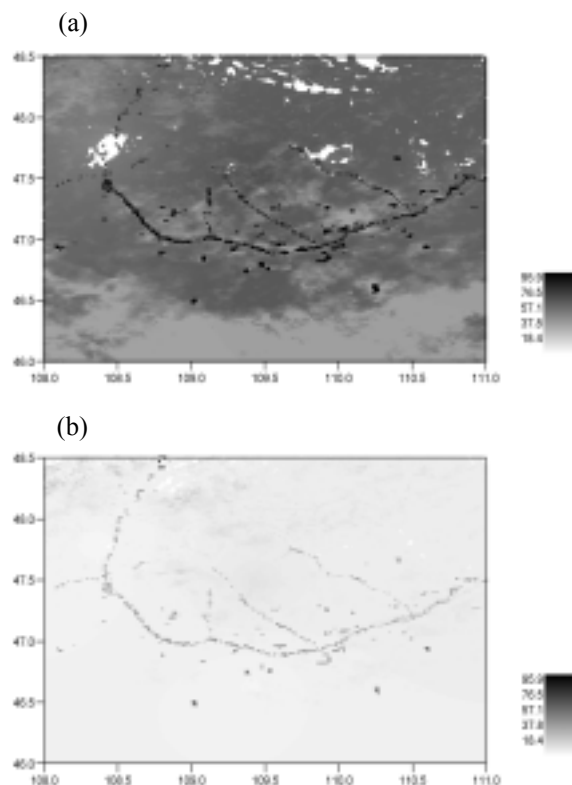


Fig. 4 Distribution of the amount of a monthly evapotranspiration in July (a) and October (b).